Compressive properties of bulk metallic glass with small aspect ratio

F.F. Wu and Z.F. Zhang[a)]
Shenyang National Laboratory for Materials Science, Institute of Metal Research, Chinese Academy of Sciences, Shenyang 110016, China

S.X. Mao
Shenyang National Laboratory for Materials Science, Institute of Metal Research, Chinese Academy of Sciences, Shenyang 110016, China; and Department of Mechanical Engineering, University of Pittsburgh, Pittsburgh, Pennsylvania 15261

The quasi-static compressive deformation behavior of a Vitreloy 1 bulk metallic glass (BMG) with an aspect ratio of 0.25 was investigated. It is found that the friction and the confinement at the specimen–loading platen interface will cause the dramatic increase in the compressive load, leading to higher compressive strength. In particular, the BMG specimens show great plastic-deformation ability, and plenty of interacted, deflected, wavy, or branched shear bands were observed on the surfaces after plastic deformation. The formation of the strongly interacted, deflected, wavy, or branched shear bands can be attributed to the triaxial stress state in the glassy specimens with a very small aspect ratio.

I. INTRODUCTION

Due to their excellent physical, chemical, and mechanical properties, bulk metallic glasses (BMGs) have sparked wide interest in the past several decades. As far as mechanical properties are concerned, BMG is characterized by high strength and high elastic strain limit, which make BMGs the potential candidates for use as engineering materials.[1–4] Under unconstrained conditions, however, almost all BMGs confront a fateful problem in that they usually fail by the formation of highly localized shear bands, leading to catastrophic failure without obvious macroscopic plasticity.[5,6] This kind of quasi-brittle deformation behavior has seriously limited the application of BMGs as engineering materials. To improve the ductility and overcome the catastrophic failure, the monotonic propagation of localized shear bands must be constrained. Therefore, BMG composites, reinforced by all kinds of wire, fiber, or particles, were produced.[7–9] Recently, ductile metal reinforced BMG composites were successfully fabricated via an effective in situ processing method.[10–12] These BMG composites exhibit large compressive, or even some tensile plastic strains, and strongly improved impact toughness compared with other BMG materials. Multiple shear bands are formed in the BMG matrix so that the catastrophic instability along the localized primary shear band can be avoided by the ductile metal phases.[8]

However, in contrast with a great amount of work on the BMG matrix composites, some attention was also paid to the interesting deformation phenomena in the monolithic BMG under geometrical constrain or under the stress state in a softer mode.[5,13–15] BMG foam is a new application for BMG family, which displays great plasticity, up to 80% without macroscopic fracture, and good ability of energy absorption under compression.[16,17] Zirconium-based BMG specimens with small aspect ratios[14,15] also display predominant compressive plasticity, surprisingly reaching 80% without catastrophic fracture, which is significantly higher than the reported data for the standard BMG specimens with an aspect ratio of 2. When subjected to cold rolling, the BMG specimens can undergo great deformation with a plasticity up to 70%,[18] leading to a significant increase in the yield stress and elastic strain at yield point. Recently, Conner et al.[13] found that thin metallic glassy ribbons showed ductility without failure in bending, but thicker plates failed catastrophically. Another possible way to trigger the formation of multiple shear bands is to apply confining pressure to the BMG specimens. In this case, Davis and Kavesh,[19] Lewandowski and Lowhaphandu,[20] and Lu and Ravichandran[21] have investigated the effect of hydrostatic pressure on the flow and fracture behavior of Zr-based metallic glasses. They found that those BMGs can exhibit large inelastic deformation of more than 10% under confinement. In addition, Bruck et al.[5] investigated the effect of two aspect ratios (0.5 and 2) on the compressive properties and found that specimens with small aspect ratio (0.5) showed a slight increase in

the yield strength and obvious increase in the compressive plasticity compared with the specimens with a normal aspect ratio of 2. Recently, Sunny et al.[22,23] also studied the dynamic compressive behavior of a Zr-based BMG with aspect ratios of 0.5, 1, and 2 and found similar results even at high strain rate. This indicates that the observed ductility of BMGs strongly depends on the specimen geometry and the applied loading modes. However, it is not quite clear how the shear bands form, develop, and interact with each other when a BMG specimen is subjected to a confined loading. In the present work, we use the specimens with a small aspect ratio of 0.25, which is far smaller than those applied by others, to further reveal the effects of small aspect ratio on yield strength and compressive plasticity as well as on the formation and evolution mechanisms of shear bands for a Zr-based BMG (Vitreloy 1), a trademark of Liquidmetal Technologies, Lake Forest, CA.

II. EXPERIMENTAL

Ingots with the composition of $Zr_{41.2}Ti_{13.8}Cu_{12.5}Ni_{10}Be_{22.5}$ (Vitreloy 1) were prepared by arc melting a mixture of pure elements in a Ti-gettered argon atmosphere on a water-cooled copper plate. The ingots were then remelted several times until a homogeneous melt was formed. The final ingots are rectangular with a dimension of $50 \times 6 \times 4$ mm^3 (length, height, and width). The microstructures and the phases of the prepared ingots were characterized using a Leo Supra 35 (Carl Zeiss, Oberkochen, Germany) scanning electron microscope (SEM), as well as by a Rigaku (Tokyo, Japan) diffractometer with Cu K$_\alpha$ radiation. The final ingots show only broad diffraction maxima, and no peaks of crystalline phases can be seen, revealing the amorphous structure of the samples. Uniaxial compressive tests were performed on the Vitreloy 1 BMG specimens with a MTS810 (MTS Systems Corporation, Eden Prairie, MN) testing machine at room temperature. All the lateral surfaces of each specimen were polished by 1.5 μm diamond paste. The final dimensions of the specimens were 1 mm in height with a 4×4 mm^2 rectangular cross section. The compression specimens were sandwiched between two polished tungsten carbide (WC) plates in a loading fixture designed to guarantee uniaxial loading. No lubricant was applied onto the contacting surfaces of the specimens. All compressive tests were conducted using a constant strain rate of about 5×10^{-4} s^{-1} and were repeated at least three times. After mechanical tests, the specimens were observed by SEM to reveal the deformation features.

III. RESULTS

A. Compressive stress-strain curves

Figure 1(a) shows the compressive engineering stress-strain curves of the BMG specimens deformed up to
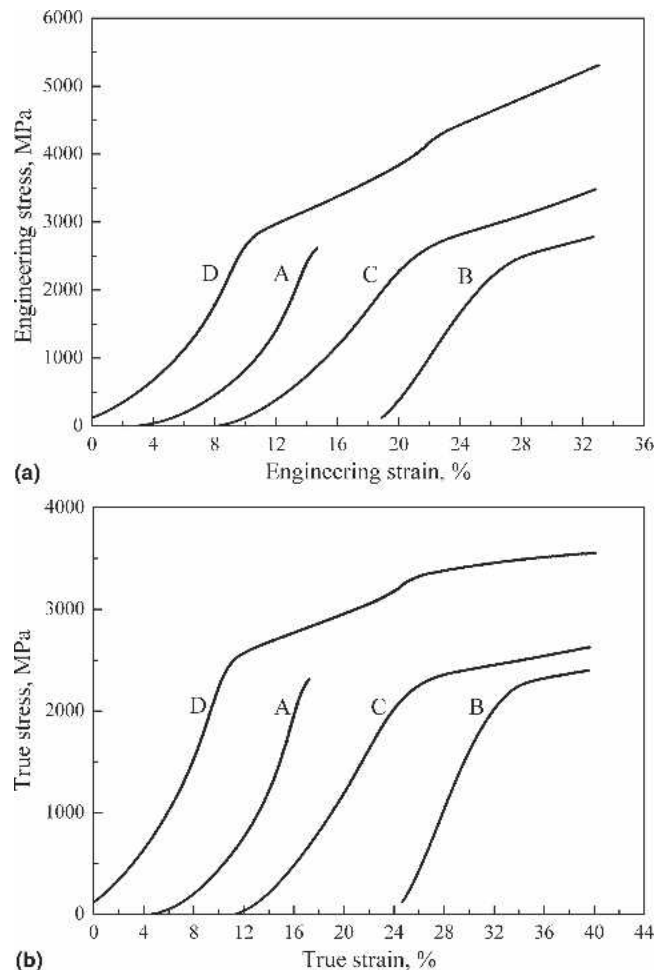

FIG. 1. Compressive engineering stress–strain curves (a) and true stress–strain curves (b) of the Vitreloy 1 specimens with an aspect ratio of 0.25 at a constant strain rate of 5×10^{-4} s^{-1}.

different strain extent of 0.6, 7.3, 13.4, and 26.9% for specimens A, B, C, and D, respectively. It is clear that when the aspect ratio is small, it is difficult to accurately measure the Young's moduli according to the aforementioned stress–strain curves, because the unevenness of the platen can affect it dramatically. However, the yielding strengths are easy to measure from the stress–strain curves and have almost the same value of 2415 MPa, which is much higher than that (1860 MPa) of the Vitreloy 1 specimens with an aspect ratio of 2.[24,25] Another feature is that its compressive plasticity can be improved to a very high value. For example, when the compressive plasticity reaches 26.9%, the specimen does not fail with catastrophic fracture, which is basically identical with the other BMG specimens with the aspect ratio smaller than 1.[14,15] It seems that there is a great work hardening observable in the engineering stress–strain curves. The flow stress of the BMG specimen D continuously increases with the plastic strain increasing from the yielding strength (2721 MPa) to a high level of 5306 MPa without

failure. To understand this strong work-hardening phenomenon, the true stress–strain curves of all the metallic glass specimens are plotted in Fig. 1(b). It can be clearly seen that the specimens still display great work hardening; the true flow stress can increase from the yield strength of 2415 to 3553 MPa, which is higher than the failure strength of Vitreloy 1 BMG under uniaxial compression. This work-hardening phenomenon in the specimen with aspect ratio of 0.25 is quite different from the data reported for other BMG specimens with aspect ratios larger than 0.5, which did not display any obvious work-hardening feature.[14] It is noted that when the specimen's aspect ratio is far smaller than 1, the friction at the specimen–loading platen interface will increase greatly, leading to higher deformation force and compressive strength.

B. Deformation features

Figure 2 shows two typical SEM macroscale images for the specimens with plastic strains of 0.6 and 26.9%. As is well known, BMG specimens with an aspect ratio of 2 normally fail in a pure shear mode.[26] However, for the specimens with small aspect ratio of 0.25, no failure
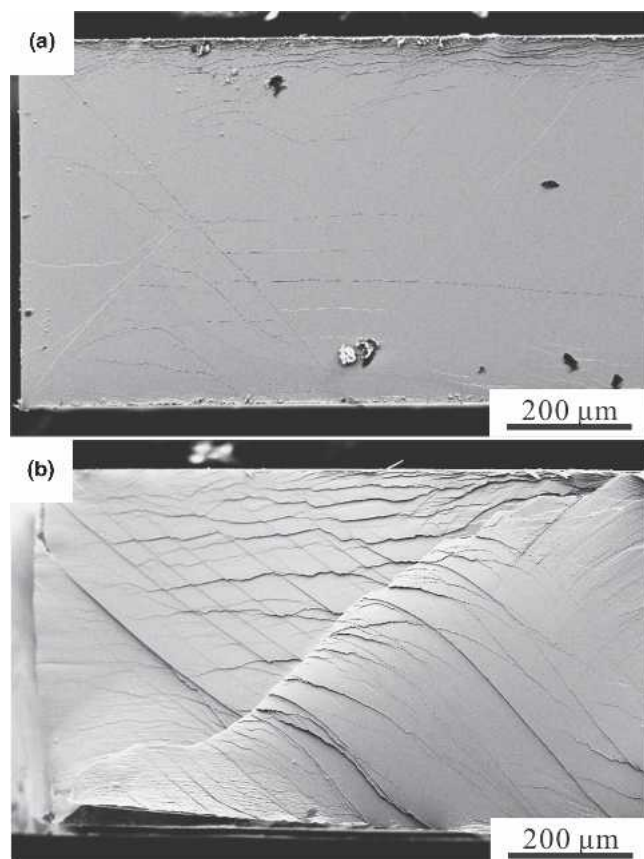

FIG. 2. Two typical macroscopic SEM images of the Vitreloy 1 specimens with aspect ratio of 0.25 undergoing (a) 0.6% and (b) 26.9% plastic deformation.

takes place with catastrophic fracture.[14,15] On the lateral surface of the specimen A with a plasticity of 0.6%, a few shear bands can be clearly observed, as shown in Fig. 3(a). The angle between the primary shear band plane and the load axis is about 42°, slightly smaller than 45°. With the extent of plastic deformation up to 7.3% [Fig. 3(b)], except for the dense primary shear bands, there are also many secondary shear bands forming from the other direction. The primary shear bands are intersected by the secondary ones, leading to a considerable plastic strain without catastrophic failure. An average shear offset of 4 μm is very easy to distinguish on the lateral surface after deformation. When the extent of plastic deformation increases further to 13.4%, the intersection or interaction between the primary and secondary shear bands becomes serious, as shown in Fig. 3(c). It is notable that plenty of branching occurs in the individual shear band. The branch of shear band is much smaller than an individual unbranched shear band. When the specimen D is compressed to a plastic strain of 26.9%, the interaction and branching of the shear bands become more serious than those in the specimens A, B, and C with small plastic deformation [Fig. 3(d)]. According to the intersection between the primary and secondary shear bands, the shear offset is measured to be about 5.7 μm on average, which is larger than that in the specimen A under a plastic strain of 0.6%.

Figure 4 shows the dependence of the spacing of primary shear bands (PSBs) on the applied plastic strain. The spacing of PSBs is on average 49.2 μm for the specimen A with a plastic strain of 0.6%. When the plastic strain increases to 7.3% and 13.4%, the spacing of PSBs obviously decreases to 30 μm and 21.2 μm, respectively. However, when the plastic strain increases to 26.9%, the spacing of PSBs is 20 μm on average, which is nearly the same as that for the specimen C with a plastic strain of 13.4%. This indicates that the spacing of PSBs has a weak dependence on the applied plastic strain at a high strain level. It seems that the PSBs will become saturated at a certain plastic strain level, and the further high plastic deformation is mainly provided by those secondary shear bands or branching of the PSBs. In other words, the density of PSBs will achieve a constant, or PSBs cannot continue to increase without limit. With further deformation, however, the secondary shear bands will generate from another direction. When they run across the PSBs, they will interact with each other, and leave evidence of shear setoff on the lateral surfaces. The shear setoff is in the order of 5 μm for the specimen D.

Besides the common straight shear bands, there are several other types of shear bands that occur when the present BMG specimens are subjected to a confined loading. One is the deflected shear bands, whose propagating direction obviously deviates from its original one, as shown in Fig. 5(a). Another is the wavy shear bands,
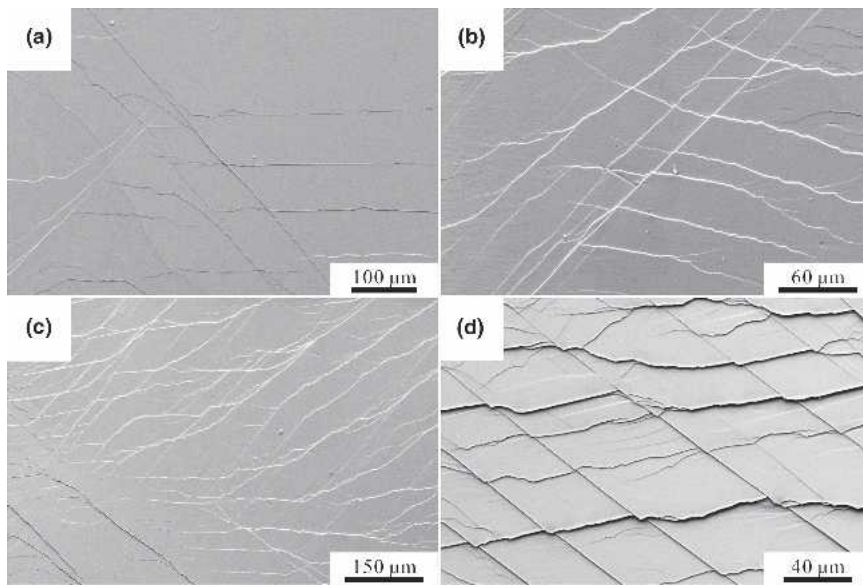
FIG. 3. SEM images of the specimens with different plastic strains of (a) 0.6%, (b) 7.3%, (c) 13.4%, and (d) 26.9%.
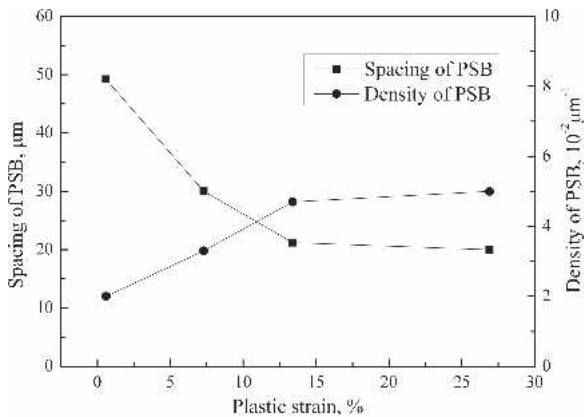

FIG. 4. The dependence of the spacing and density of PSB on the plastic strain.

which seem to propagate in a sinusoidal trace, leaving the zig-zag feature on the surfaces of the BMG specimens, as shown in Fig. 5(b). The last one is the branched shear bands, as shown in Fig. 5(c). The deflected and wavy shear bands undoubtedly have a longer path than the common straight one so that more plastic work can be dissipated during the propagation of the deflected or wavy shear bands. That is very helpful to improve the plastic-deformation ability. As far as the branched shear bands are concerned, the shear strain in any branch may be much smaller than that of an individual unbranched shear band. As a result, the branching of shear bands can effectively distribute the plastic strain homogeneously on the severe deformed region. It also dissipates more plastic work and is helpful to improve the plastic-deformation ability. Therefore, it makes it more difficult for a propagating shear band to form a catastrophic crack, and the plastic strain prior to failure is greatly improved.

In summary, the deflected, wavy, and branched shear bands join up to elongate the propagating path of the shear bands and to absorb more plastic work, leading to the predominant improvement of the plastic strain in the BMG specimens.

IV. DISCUSSION

From the experimental results described in Sec. III, it can be considered that the compressive plasticity of the BMG and the corresponding formation of multiple shear bands are strongly affected by the small aspect ratio. It is well known that the shear bands for the specimens with a normal aspect ratio of 2 are straight and usually exist as well-separated individual shear bands.[26] However, the shear bands for the present BMG specimens with a smaller aspect ratio of 0.25 are more jagged and typically occur as groups of several shear bands close together. For the BMG specimens with small aspect ratios, the shear bands terminate at the interfaces between the upper and lower surfaces of the specimens and the platens.[14,15] This indicates that the platens can effectively prevent the excessive propagation of individual shear bands, resulting in the multiplication of shear bands. During compression, besides the uniaxial stress, there is often a lateral stress induced by friction between the end of the samples and the restraint by the platen of the testing machine.[27] The two kinds of stresses will cause a hydrostatic pressure in the specimen close to the platen. Therefore, the deformation behavior of the Vitreloy 1 BMG material with smaller aspect ratio becomes complicated. The effect of the specimen geometry (aspect ratio) on the deformation behavior is discussed here.

Lu and Ravichandran[21] found that the inelastic strain is over 10% with the formation of multiple shear bands
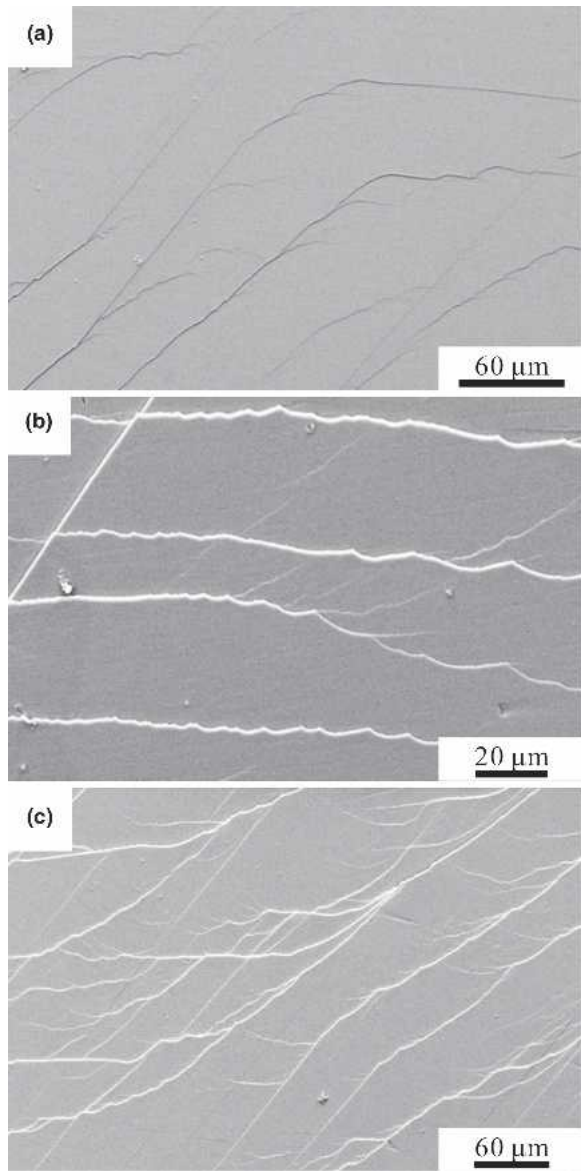
FIG. 5. Three kinds of typical shear bands in the specimens with small aspect ratio of 0.25. (a) Deflected shear bands, (b) wavy shear bands, and (c) branched shear bands.

when their Zr-based glassy samples were subjected to a lateral confinement. With further applying compressive stress, the density of the shear bands will increase continuously, resulting in a high compressive plasticity, as shown in Fig. 2. Sunny et al.[23] reported that as the aspect ratio is lowered, the strains to failure appear to increase substantially at high strain rate because the absence of a dominant shear band leads to shear banding that is more diffused and multiple shear bands are observed leading to a relatively higher strain to failure. For a better understanding of the effect of the aspect ratio on the deformation behavior of the present compressive specimens, a new model is proposed to illustrate the effect of the aspect ratio of the cylinder specimen on deformation

features, as shown in Figs. 6 and 7. When compressing the cylinder specimen, one gets two primary cones by drawing two isosceles right triangles, whose two right sides make angles of about 45° with the loaded
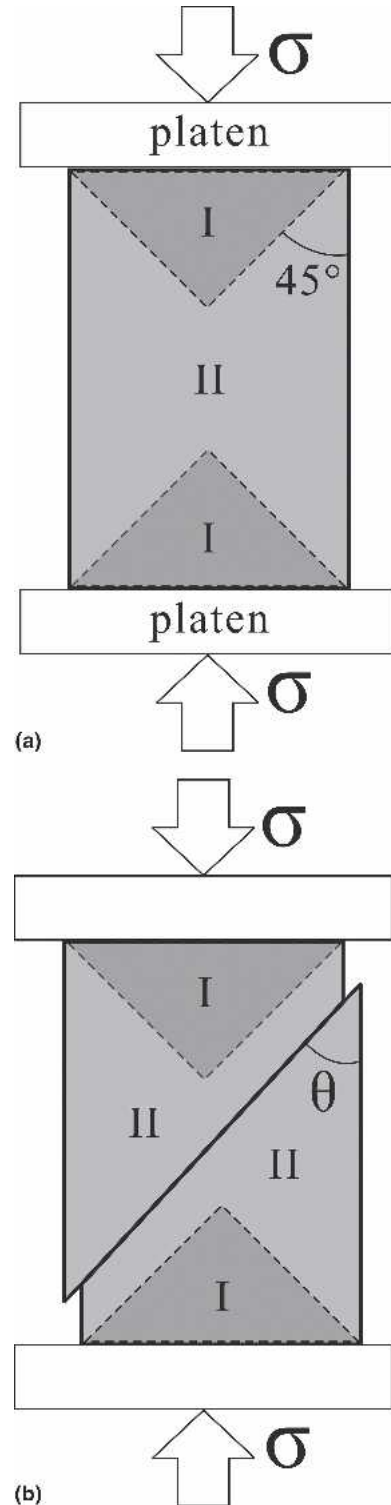

FIG. 6. Illustration of (a) weak confining effect of the platen and (b) the shear fracture mode for the specimen with aspect ratio of 2 under compression.
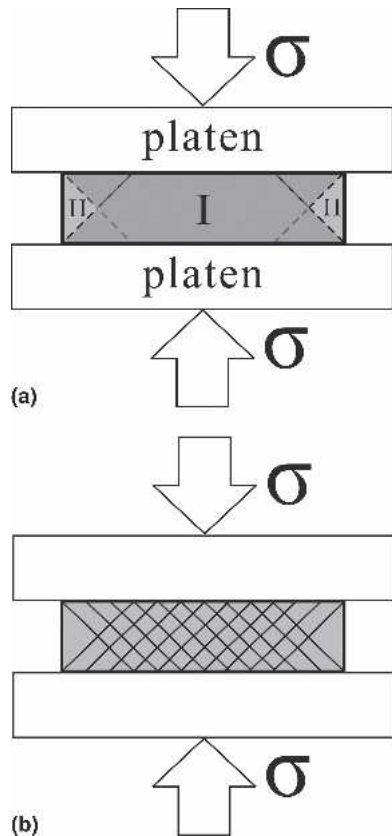
FIG. 7. Illustration of (a) strong confining effect of the platen and (b) the formation of multiple shear bands for the specimen with a smaller aspect ratio of 0.25 under compression.

compressive pressure [Fig. 6(a)].[28] Therefore, two regions are formed in the specimen: one is region I, the difficult deformation region inside the cone; the other is region II, the easy deformation region outside the cone. Due to the high hydrostatic pressure caused by the platen, region I needs large force and much energy to deform. However, region II is far away from the platen and is relatively easy to deform because the influence of hydrostatic pressure is relatively smaller than that in region I. For a BMG specimen with a normal aspect ratio of 2, the easy deformation region II is larger than the difficult deformation region I, so the constraint of the platen is very slight, which often leads to the catastrophic fracture by the fast propagation of a localized primary shear bands, as shown in Fig. 6(b). With decreasing the aspect ratio to far below 1, such as 0.25 in the present specimens, the upper and lower region I are united as one big difficult deformation region I, which is obviously larger than region II, the easy deformation region. Therefore, higher pressure and more energy are required to make the specimen deform, which is the reason why the yield stress (average 2415 MPa) of the present specimen with small aspect ratio is clearly higher than that (1860 MPa) of the BMG specimens with the aspect ratio close to

2.[24,25] Though the yield stress increases greatly, due to the merging of the upper and lower region I, it is notable that the deformation becomes more homogeneous; therefore, interacted multiple shear bands can be easily observed on the full surfaces of the specimens after compressive deformation. Moreover, a local stress fluctuation seems to exist, leading to the formation of deflected and wavy shear bands, as shown in Figs. 5(a) and 5(b). Based on the investigation on the branching of the shear bands, it might be possible that the whole region of an individual shear band could become a potential source to stimulate the new branches of shear bands [Fig. 5(c)].

Chen et al.[29] estimated that the shear strain within the shear bands is as high as 10^2–10^3, so the shear bands have the outstanding capability to accommodate large plastic strains, which may be attributed to the metallic-bonding nature of metallic glasses. If the strain can be dispersed into the multiple shear bands, so as to alleviate the strain localization in individual shear bands, metallic glasses, including BMGs, can avoid brittle fracture and exhibit their high intrinsic ductility. In fact, this idea has been realized by the development of the ductile secondary phases or ceramic-reinforced BMG composites.[7–9] The current research further demonstrates that the geometrical constraints can also prevent the excessive propagation of individual shear band in localized regions and promote the multiplication of the shear bands, resulting in sufficient development of plastic deformation. The present results demonstrate that the Vitreloy 1 BMG is intrinsically ductile because it can accommodate very high plastic deformation through the formation of the strongly interacted, deflected, wavy, or branched shear bands under the triaxial stress state. However, some intrinsically brittle BMGs, for example, Co- or Mg-based BMGs, often break into many small particles or powders under compression even with a very small aspect ratio.[30] The intrinsically brittle or ductile failure can be attributed to difference in the parameter $\alpha = \tau_0/\sigma_0$ for different BMGs, which has been discussed elsewhere.[30,31]

V. CONCLUSIONS

The deformation behavior of the Vitreloy 1 BMG specimens strongly depends on their geometry, such as aspect ratio. When the specimen's aspect ratio decreases to be far smaller than 1, such as 0.25, the friction at the specimen–loading platen interface will cause a dramatic increase in the compressive load, leading to higher compressive strength. The relatively small aspect ratio of the specimens results in trapping of the shear bands between the loading platens and formation of plenty of intersected, deflected, wavy, and branched shear bands, which is the reason why the Vitreloy 1 BMG specimens with an aspect ratio of 0.25 exhibit great plastic strain under compression. It is considered that the

present results would be helpful for conveniently investigating the plastic-deformation behaviors of BMG. Moreover, the present results would be greatly important in the engineering applications of BMG materials, in which the geometry of components made of BMG materials should be considered to achieve the balance between the strength and ductility of BMGs.

ACKNOWLEDGMENTS

REFERENCES

1. A. Inoue: Stabilization of metallic supercooled liquid and bulk amorphous alloys. *Acta Mater.* **48,** 279 (2000).
2. J.F. Löffler: Bulk metallic glasses. *Intermetallics.* **11,** 529 (2003).
3. W.H. Wang, C. Dong, and C.H. Shek: Bulk metallic glasses. *Mater. Sci. Eng. R* **44,** 45 (2004).
4. A.I. Salimon, M.F. Ashby, Y. Brechet, and A.L. Greer: Bulk metallic glasses: What are they good for? *Mater. Sci. Eng., A* **375–377,** 385 (2004).
5. H.A. Bruck, T. Christman, A.J. Rosakis, and W.L. Johnson: Quasi-static constitutive behavior of $Zr_{41.25}Ti_{13.75}Ni_{10}Cu_{12.5}Be_{22.5}$ bulk amorphous-alloys. *Scripta Metall. Mater.* **30,** 429 (1994).
6. H.A. Bruck, A.J. Rosakis, and W.L. Johnson: The dynamic compressive behavior of beryllium bearing bulk metallic glasses. *J. Mater. Res.* **11,** 503 (1996).
7. H. Choi-Yim and W.L. Johnson: Bulk metallic glass matrix composites. *Appl. Phys. Lett.* **71,** 3808 (1997).
8. R.D. Conner, R.B. Dandliker, and W.L. Johnson: Mechanical properties of tungsten and steel fiber reinforced $Zr_{41.25}Ti_{13.75}Cu_{12.5}Ni_{10}Be_{22.5}$ metallic glass matrix composites. *Acta Mater.* **46,** 6089 (1998).
9. D.H. Bae, M.H. Lee, D.H. Kim, and D.J. Sordelet: Plasticity in $Ni_{59}Zr_{20}Ti_{16}Si_2Sn_3$ metallic glass matrix composites containing brass fibers synthesized by warm extrusion of powders. *Appl. Phys. Lett.* **83,** 2312 (2003).
10. C.C. Hays, C.P. Kim, and W.L. Johnson: Microstructure controlled shear band pattern formation and enhanced plasticity of bulk metallic glasses containing in situ formed ductile phase dendrite dispersions. *Phys. Rev. Lett.* **84,** 2901 (2000).
11. G. He, J. Eckert, and W. Löser: Stability, phase transformation and deformation behavior of Ti-base metallic glass and composites. *Acta Mater.* **51,** 1621 (2003).
12. F.F. Wu, Z.F. Zhang, A. Peker, S.X. Mao, J. Das, and J. Eckert: Strength asymmetry of ductile dendrites reinforced Zr- and Ti-based composites. *J. Mater. Res.* **21,** 2331 (2006).
13. R.D. Conner, Y. Li, W.D. Nix, and W.L. Johnson: Shear band spacing under bending of Zr-based metallic glass plates. *Acta Mater.* **52,** 2429 (2004).
14. Z.F. Zhang, H. Zhang, X.F. Pan, J. Das, and J. Eckert: Effect of aspect ratio on the compressive deformation and fracture behaviour of Zr-based bulk metallic glass. *Philos. Mag. Lett.* **85,** 513 (2005).
15. H. Bei, S. Xie, and E.P. George: Softening caused by profuse shear banding in a bulk metallic glass. *Phys. Rev. Lett.* **96,** 105503 (2006).
16. A.H. Brothers and D.C. Dunand: Syntactic bulk metallic glass foam. *Appl. Phys. Lett.* **84,** 1108 (2004).
17. A.H. Brothers and D.C. Dunand: Plasticity and damage in cellular amorphous metals. *Acta Mater.* **53,** 4427 (2005).
18. Y. Yokoyama, K. Yamano, K. Fukaura, H. Sunada, and A. Inoue: Enhancement of ductility and plasticity of $Zr_{55}Cu_{30}Al_{10}Ni_5$ bulk glassy alloy by cold rolling. *Mater. Trans.* **42,** 623 (2001).
19. L.A. Davis and S. Kavesh: Deformation and fracture of an amorphous metallic alloy at high pressure. *J. Mater. Sci.* **10,** 453 (1975).
20. J.J. Lewandowski and P. Lowhaphandu: Effects of hydrostatic pressure on the flow and fracture of a bulk amorphous metal. *Philos. Mag. A* **82,** 3427 (2002).
21. J. Lu and G. Ravichandran: Pressure-dependent flow behavior of $Zr_{41.2}Ti_{13.8}Cu_{12.5}Ni_{10}Be_{22.5}$ bulk metallic glass. *J. Mater. Res.* **18,** 2039 (2003).
22. G.P. Sunny, V. Prakash, and J.J. Lewandowski: Results from a novel insert design for high strain-rate compression of a bulk metallic glass, in *Proceedings of the 2006 International Mechanical Engineering Conference and Exposition* (American Society of Mechanical Engineers, New York, NY, 2006).
23. G.P. Sunny, F. Yuan, J.J. Lewandowski, and V. Prakash: Dynamic stress-strain response of a Zr-based bulk metallic glass, in *Proceedings of the 2005 SEM Annual Conference and Exposition on Experimental and Applied Mechanics* (Society of Experimental Mechanics, Bethel, CT, 2005).
24. G. Subhash, R.J. Dowding, and L.J. Kecskes: Characterization of uniaxial compressive response of bulk amorphous Zr-Ti-Cu-Ni-Be alloy. *Mater. Sci. Eng., A* **334,** 33 (2002).
25. J. Lu, G. Ravichandran, and W.L. Johnson: Deformation behavior of the $Zr_{41.2}Ti_{13.8}Cu_{12.5}Ni_{10}Be_{22.5}$ bulk metallic glass over a wide range of strain-rates and temperatures. *Acta Mater.* **51,** 3429 (2003).
26. Z.F. Zhang, J. Eckert, and L. Schultz: Difference in compressive and tensile fracture mechanisms of $Zr_{59}Cu_{20}Al_{10}Ni_8Ti_3$ bulk metallic glass. *Acta Mater.* **51,** 1167 (2003).
27. Z.F. Zhang, D. Brunner, C. Scheu, and M. Rühle: Deformation and fracture mechanisms of $Al_2O_3/Nb/Al_2O_3$ composites under compression. *Z. Metallkd.* **96,** 62 (2005).
28. B. Avitzur: *Handbook of Metal Forming* (John Wiley & Sons, New York, 1983).
29. H. Chen, Y. He, G.J. Shiflet, and S.J. Poon: Deformation-induced nanocrystal formation in shear bands of amorphous-alloys. *Nature* **367,** 541 (1994).
30. Z.F. Zhang, H. Zhang, B.L. Shen, A. Inoue, and J. Eckert: Shear fracture and fragmentation mechanisms of bulk metallic glasses. *Philos. Mag. Lett.* **86,** 643 (2006).
31. Z.F. Zhang and J. Eckert: Unified tensile fracture criterion. *Phys. Rev. Lett.* **94,** 094301 (2005).